Journal of Chromatography A, 1217 (2010) 7898–7906

Contents lists available at ScienceDirect

Journal of Chromatography A

journal homepage: www.elsevier.com/locate/chroma

Physicochemical characterization of dilute n-alcohol/biodiesel mixtures by inverse gas chromatography

N. Scott Bobbitt, Jerry W. King*

Department of Chemical Engineering, University of Arkansas, 3202 Bell Engineering Center, Fayetteville, AR 72701, USA

ARTICLE INFO

Article history:
Received 8 July 2010
Received in revised form
12 September 2010
Accepted 12 October 2010
Available online 20 October 2010

Keywords:
Activity coefficients
Biodiesel
Gas chromatography
Inverse
Isotherms
Thermodynamics

ABSTRACT

Inverse gas chromatography (IGC) has been used to determine the physicochemical parameters that characterize solution thermodynamic interactions in biodiesel–n-alcohol solute systems. Such data is of value to chemical engineers and separation scientists in optimizing separation processes to separate alcoholic solutes at low concentrations in soybean oil methyl ester mixtures (biodiesel). The derived activity and Henry's Law coefficient data can be used to rationalize the interaction of four members of an n-alcoholic homologous series and the soya-based methyl ester solvent in terms of such esters as "green" renewable solvents. Sorption isotherm data confirm linear behavior in most cases between the solute (alcohol) vapor state concentrations and their uptake into the biodiesel phase. Overall, the experimentally determined activity coefficients agree well with those predicted by solution thermodynamic theories as well as correlative chemical engineering equations.

1. Introduction

Recent years have seen a sharp increase in the production of biodiesel for a renewable source of energy in an effort to reduce fossil fuel dependence. Biodiesel is a mixture of alcoholic esters, predominantly methyl esters, produced by the transesterification of triglyceride-based feedstocks such as vegetable oils and animal fats. Glycerol is produced as a byproduct of this reaction, and residual alcohol may be left in the product ester. Methanol is the most common alcohol used in making commercial biodiesel [1,2]. The excess alcohol and the glycerol must be separated from the ester to yield high-purity biodiesel, typically using a centrifugal or distillation separation process.

Outside of the bioenergy sector, alkyl esters are also used as "green" solvents and intermediates in the production of other oleochemicals, *id est* chemicals derived from plant and animal fats [3]. An example of such a function is the use of biodiesel as an environmentally friendly solvent to remove crude oil from sandy beaches resulting from accidental oil spills [4]. Biodiesel has also been used as a solvent to facilitate removal of butanol from aqueous solution [5]. These applications require knowledge of the solution and physicochemical properties of the esters; however, these data are currently limited in the literature.

Inverse gas chromatography (IGC) is an inexpensive and effective way to measure physicochemical properties such as sorption isotherms, Henry's Law constants, and activity coefficients [6–8]. IGC has been used extensively to characterize a variety of stationary phases such as polymers [9–14], a plethora of studies on ionic liquids [15–20], surfaces and interfacial chemistry [21–26], lipid substances [27,28], scrap tires [29], to nanoparticles [30,31]. Studies have been reported using oleochemical stationary phases such as soybean oil [32,33] and on soybean stock biodiesel [34].

Previous studies have been reported by Chiu et al. [35] and Felice et al. [36] to determine distribution coefficients of methanol between biodiesel and glycerin, but other industrially relevant alcohols such as n-butanol and ethanol were not studied. Methanol and ethanol in biodiesel and glycerol mixtures were studied by Zhou and Boocock [37]. Another study was recently done by Silva et al., to determine the activity coefficients of the components in ternary biodiesel–alcohol–glycerol systems using combinatorial UNIFAC predictions [38]. Kuramochi et al., have also recently published a study involving modeling biodiesel systems with UNIFAC [39]. Oliveira et al., have also modeled multicomponent biodiesel systems using cubic-plus-association equations of state [40].

This study has investigated the interactions between four n-alcohol solutes and biodiesel (as solvent) obtained from a commercial source. Specific retention volumes, activity coefficients, and Henry's Law coefficients are reported. Comparisons have been made between experimental activity coefficient data and several

* Corresponding author. Tel.: +1 479 575 5979; fax: +1 479 575 7926.
E-mail address: jwking1@uark.edu (J.W. King).

0021-9673/$ – see front matter © 2010 Elsevier B.V. All rights reserved.
doi:10.1016/j.chroma.2010.10.047

theoretical predictive methods. Sorption isotherm data were generated at finite injection concentrations using the method of Conder and Young[41] which is frequently called the Elution by Characteristic Point method (ECP). The thermodynamic data generated by IGC in this study add to our understanding of biodiesel's solvent properties, as well as providing requisite physicochemical data for the design of biodiesel purification processes.

2. Theory and calculations

Sorption isotherms were calculated using the ECP method described by Conder and Young [41]. In this method, an assumption is made that the non-equilibrium (kinetic diffusion) contribution to the peak profile occurs equally on either side of the center line of the peak, and this is subtracted from the observed asymmetry in the chromatographic peak profile to yield a profile attributed to the thermodynamic partition or sorption of solute vapor onto the column stationary phase.

The ratio of solute uptake in moles of solute per moles of stationary phase is given by

$$q = \alpha \frac{n}{\mu A_p} \tag{1}$$

where α is the area of the partition at the defined height, n is the moles of sample injected, μ is the moles of stationary phase, and A_p is the area of the chromatographic peak. α, and hence q, are found at several different heights ranging from 10% of peak height to the full peak height. The isotherm is produced by plotting this array of q-values against the corresponding array of ratios of partial pressure to vapor pressure of the solute, given by Eq. (2) as:

$$p = \frac{RnTr_A h}{A\dot{V} j_M} \tag{2}$$

where R is the gas constant, n is the number of moles of solute injected, T is column temperature, h is the height corresponding to a given ratio p/p^o, A is the total peak area, $\dot{V}$ is volumetric flow rate of carrier gas, j_M is the James-Martin compressibility factor, and r_A is the data acquisition rate in units of γ/time where γ is an arbitrary unit defined as the length associated with one data point on the abscissa of the chromatogram. The height, h, is given in units of potential, such as volts, and so the dimensions of peak area, A, are length-potential, given in units of γ-V, which then cancel with the acquisition rate and height in the numerator [42].

The specific retention volumes were calculated and corrected to 0 °C using Eq. (3) [43].

$$V_g^0 = \frac{t_0 F_c}{r_A w} \frac{273.16}{T_{col}} \tag{3}$$

Here t_0 is the peak centroid retention time, r_A is again the acquisition rate, w is the mass of the stationary phase, T_{col} is column temperature, and F_c is the corrected carrier flow rate given by Eq. (4).

$$F_c = F_a \frac{T_{col}}{T_{amb}} \left(1 - \frac{P_W}{P_a}\right) j_M \tag{4}$$

Here F_a is the carrier gas flow rate measured at ambient temperature, P_w is the vapor pressure of water at ambient temperature, P_a is the ambient pressure, and j_M is the James-Martin correction factor [41].

The Henry's Law coefficients were calculated using Eq. (5):

$$H_i = \frac{RT}{V_g^0 M_i} \tag{5}$$

where M_i is the molecular weight of the probe solute and H_i is given in units of pressure dictated by the chosen gas constant.

The mass fraction activity coefficients were calculated using Eq. (6):

$$\ln(\gamma_m^i) = \ln\left(\frac{273.16R}{V_g^0 M_i P_i^0}\right) - \frac{P_i^0(B_{11} - \bar{V}_i)}{RT} \tag{6}$$

where P^o is the vapor pressure of the solute, B_{11} is the second pure virial coefficient corresponding to the injected solute, and $\bar{V}_i$ is the molar volume of the solute. In practice the second (virial coefficient) term is very small and is often neglected, particularly when using helium as a carrier gas at the very low pressures employed in IGC experiments. (In this study the contribution from the virial term represented less than 1% of the mass fraction activity coefficient on average.) The mass fraction activity coefficient is converted to a mole fraction activity coefficient using the ratio of molecular weights of the mobile and stationary phases, in Eq. (7):

$$\gamma_x^i = \gamma_m^i \left(\frac{M_i}{\langle M_S \rangle}\right) \tag{7}$$

where M_i is the molecular weight of the solute in Da, and M_s is the molecular weight of the stationary phase—shown here as an average molecular weight of the biodiesel sample. The average molecular weight of biodiesel is approximately 292.2 Da [44].

The gas–liquid partition coefficient is defined as the ratio of net retention volume to the volume of the stationary phase [41]. This value can also be expressed as the product of the specific retention volume and the density of the stationary phase, as seen in Eq. (8).

$$K_i = V_g^0 \rho_s \tag{8}$$

The specific retention volume data were also used to calculate the Flory–Huggins interaction parameter given by Eq. (9):

$$\chi_i = \ln\left[\frac{273.16R}{V_g^0 M_i P_i^o}\right] - \frac{P_i^o(B_{11} - \bar{V}_i)}{RT} - \ln\left[\frac{v_i}{v_s}\right] + \frac{\bar{V}_i}{\langle M_s \rangle v_s} - 1 \tag{9}$$

where χ_i is the Flory–Huggins interaction parameter, v_i is the specific volume of the solute and v_s is the specific volume of the stationary (solvent) phase, though in practice the two terms containing specific volumes are often negligibly small [28].

Ashworth and Everett [45] have shown that the activity coefficient can be separated into the logarithmic sum of an entropic and enthalpic activity coefficient contributions, as seen in Eq. (10).

$$\ln \gamma = \ln \gamma^E + \ln \gamma^S \tag{10}$$

Martire [46] has described a method embracing several well-known solution thermodynamic theories for calculating the values of the aforementioned terms based on a regular solution approximation for the enthalpic term combined with the entropic term, in which $\ln \gamma^S$ are calculated using the Flory–Huggins or Miller–Guggenheim models. The enthalpic term is calculated from regular solution theory using Eq. (11)

$$\ln \gamma_i^E = \frac{\bar{V}_s}{RT}(\delta_i - \delta_S)^2 \tag{11}$$

where δ_s is the Hildebrand solubility parameter for the stationary phase. The entropic contribution is given by the general form of Eq. (12):

$$\ln \gamma^S = \ln\frac{1}{r} + \vartheta \ln\frac{6r}{5r+1} + \varphi\left(1 - \frac{1}{r}\right) \tag{12}$$

where r is the ratio of molar volumes ($\bar{V}_s/\bar{V}_i$). For the Miller–Guggenheim statistical solution thermodynamic approximation $\vartheta = 6$ and $\varphi = 0$, and in the special case of the Flory–Huggins approximation $\vartheta = 0$ and $\varphi = 1$ [46–48].

The generated IGC activity coefficient data were used to calculate the binary interaction parameters (A_{ij} and A_{ji}) that govern the two-constant Margules equation, which is an activity coefficient

predictive method that is based random mixing, shown in Eq. (13) [49].

$$\ln \gamma_i = x_j^2[A_{ij} + 2(A_{ji} - A_{ij})x_i] \quad (13)$$

3. Materials and methods

The IGC experiments were done using a simple, but modified Gow-Mac Model 550 gas chromatograph equipped with a thermal conductivity detector. Ultra-high-purity helium was used as a carrier gas, and the carrier flow rate was measured using a soap bubble flow meter at the exit port of the column [50]. A mercury manometer inserted into the front of the system which was used to determine the inlet pressure, and a mercury barometer (Fisher Scientific, Pittsburgh, PA) nearby was used to measure the ambient pressures.

Column temperatures were measured using three J-type thermocouples wrapped tightly around the column at different points, and the three temperature readings from the thermocouples were averaged in reporting the column temperature. A fourth J-type thermocouple was used to read the ambient temperature. All thermocouple signals were transmitted to a Dell Inspiron 1420 laptop computer through a Cole-Parmer® (Vernon Hills, IL) data acquisition board (Model # 18200-40) and recorded using TracerDAQ©, which then allowed the data to be exported to Excel©. The thermal conductivity detector signal from the GC unit was also transmitted through a Cole-Parmer® digitization board (Model # 18200-00) to the TracerDAQ© software. The signal from the detector was amplified by a factor of 100 by a voltage amplifier that was constructed in-house.

The IGC columns were constructed from 80 cm sections of 1/4″ (outer diameter) copper tube filled with Chromosorb® GAW/DMDCS 45–60 mesh silyated diatomaceous earth packing (#25651, Lot 309, ResTek Corporation, Bellefonte, PA) coated with biodiesel (B99 Biodiesel, 5/28/09, soybean stock, NREL, Golden, CO) using a rotary evaporator (Model IKA12-V10, VWR Scientific, West Chester, PA) to achieve approximately 16, 20, and 25% by mass liquid phase loadings relative to the weight of the Chromosorb® GAW used to make the column packings. Columns were packed with the aid of a vibrator and vigorous tapping, the GC support material being held in the column by silanized glass wool plugs at each end.

A 10 or 20 μL Hamilton syringe (Hamilton Company, Reno, NV) was used to manually inject the solute samples, along with ~5 mL dead volume of air (to measure the void volume of the column). When each injection was made, a tap key connected to a standard AA battery (1.5 V) was pressed to send a sharp signal to the data acquisition software and denote the injection time on the peak profile. A detector current of 230 mA was used for all experiments, and the detector temperature was held at 230 °C. The column temperatures employed ranged from 55 °C to 85 °C with injection port temperature ranging from 5 to 15 °C above the respective column temperatures. The four solutes tested were methanol, ethanol, n-propanol, and n-butanol, using injection volumes of 4, 7, and 10 μL for each alcohol. All alcohols were ACS grade. Methanol, n-propanol, and n-butanol were obtained from VWR Chemicals (Batavia, IL, Prod. ## MX0475-1, PX1824-6, and BX1780-6 respectively). Ethanol was obtained from PharmCo Product, Inc. (Brookfield, CT, CAT # E200).

Data reduction was done primarily using a MATLAB© routine written in-house and Microsoft Excel©.

4. Results and discussion

4.1. Detector linearity

The height and area of the resultant profiles from injections of differing sizes were plotted against injection volume to determine if the detector was providing a linear response. Peak height and peak area varied linearly with injection volume with regression coefficients of 0.9881 and 0.999 respectively. These are shown in Fig. 1(a and b) along with the linear regression equations for peak height and peak area versus injection size.

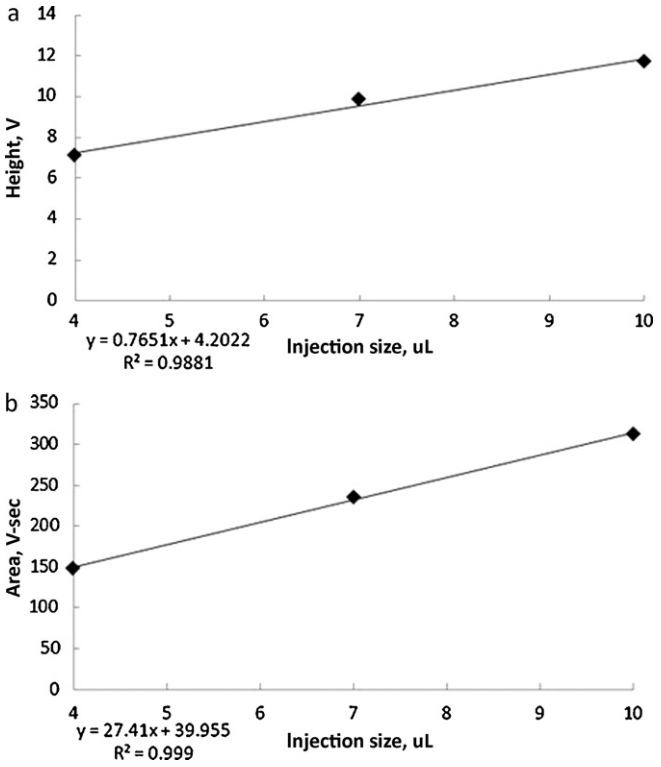

Fig. 1. (a) Plot of peak height vs. injection volume for ethanol using the thermal conductivity detector and corresponding regression equation.(b) Plot of peak area vs. injection volume for ethanol using thermal conductivity detector and corresponding regression equation.

4.2. Experimental repeatability

Injections were performed in triplicate for a representative range of solutes and temperatures to demonstrate the precision and repeatability of these techniques, and the remaining injections were performed singly. For those samples performed in triplicate the average coefficient of variation in the measured retention time was 0.038, the average coefficient of variation in the measured peak profile heights was 0.007, and the average coefficient of variation in the measured peak areas was 0.017. This agreement is considered excellent.

The mass loading of the column packing was determined via pyrolysis before and after each set of injections. On average 7.5% of the biodiesel packing was lost during the experiments; the average loading for each column was used for all subsequent calculations.

The density of the biodiesel as a function of temperature was calculated using data from Tate et al. [51].

4.3. Specific retention volumes and related data

The specific retention volumes for each injected solute and temperature were calculated using Eq. (4). The average values for the specific retention volumes as well as Henry's Law constants (Eq. (6)), partition coefficients (Eq. (9)), and Flory–Huggins interaction parameters (Eq. (10)) are reported below in Tables 1–4.

As shown in Table 1, the specific retention volumes for all alcohols decrease as the temperature increases, which is a reflection

Table 1
Specific retention volumes of n-alcohol solutes on biodiesel columns over the temperature range (56.7–85.3 °C).

Specific retention volume (mL/g)	Temperature (°C)			
	56.7	65.1	75.7	85.3
Methanol	34.0	23.6	16.6	12.6
Ethanol	77.5	56.3	38.0	27.3
Propanol	211.5	160.5	112.1	78.6
Butanol	562.2	429.5	288.9	199.8

Table 2
Solute Henry's Law coefficients as a function of temperature (56.7–85.3 °C) and alcohol (n-C_1–C_4) type.

Henry's Law Constant (atm)	Temperature (°C)			
	56.7	65.1	75.7	85.3
Methanol	25.18	36.81	54.04	73.13
Ethanol	7.65	10.74	16.44	23.42
Propanol	2.14	2.89	4.28	6.25
Butanol	0.65	0.88	1.35	2.00

Table 3
n-Alcohol partition coefficients in to biodiesel as a function of temperature (56.7–85.3 °C) and alcohol type.

Partition coefficient	Temperature (°C)			
	56.7	65.1	75.7	85.3
Methanol	29.2	20.2	14.1	10.7
Ethanol	65.9	47.9	32.3	23.2
Propanol	179.8	136.4	95.3	66.8
Butanol	477.9	365.1	245.5	169.8

of the increased volatility of the solutes and decreased interaction between the solutes and the soybean oil methyl ester (biodiesel) stationary phase.

The specific retention volumes also increase as the carbon number of the alcohol increases. This suggests that higher molecular weight alcohols absorb more readily into the biodiesel. Based on this observation, it would be expected that alcohols with longer carbon chains will exhibit even more absorption and lower activity coefficients (lower escaping tendencies) than alcohols with short carbon chains from the biodiesel solvent.

4.4. Activity coefficients

4.4.1. Experimental results and trends

The magnitude of the solute activity coefficients depends on both temperature and composition, *id est* solute concentration in the biodiesel solvent. There is some data in the literature only at infinitely dilute conditions for the solute in biodiesel or a model solvent, and theoretical predictive calculations apply only to these infinitely dilute conditions. The purpose of this study was to examine alcohol–biodiesel systems at higher alcohol concentrations; however, it should be noted that the range of compositions examined in this study is still relatively small and fairly close to infinite dilution (0.5–4.5 mol%alcohol). For the purpose of comparing them to published data, the activity coefficients were averaged for each temperature over the small range of compositions that approached infinite dilution. Other predictive methods (see below) that account for the compositional dependence of the activity coefficient were also examined, and those comparisons were made at the proper solution compositions accordingly. These averaged activity coefficients are tabulated in Table 5 on a mole fraction basis and were calculated using Eq. (7), including the second virial coefficient term, which many investigators neglect.

Table 4
Flory–Huggins interaction parameters for the n-alcohol/biodiesel systems as a function of temperature and alcohol type.

Flory–Huggins χ parameter	Temperature (°C)			
	56.7	65.1	75.7	85.3
Methanol	2.38	2.41	2.36	2.30
Ethanol	1.81	1.77	1.74	1.71
Propanol	1.41	1.30	1.20	1.17
Butanol	1.28	1.10	0.98	0.91

Table 5
Molar fraction activity coefficients of n-alcohols (n-C_1–C_4) as a function of temperature.

Activity coefficient	Temperature (°C)			
	56.7	65.1	75.7	85.3
Methanol	3.16	3.21	3.06	2.86
Ethanol	2.42	2.32	2.25	2.17
Propanol	1.97	1.76	1.60	1.54
Butanol	2.02	1.69	1.49	1.38

Note as the temperature increases, the alcoholic solutes enter solution with the biodiesel more readily, *id est* they exhibit a lower escaping tendency that corresponds to a lower activity coefficient. This seems to be the opposite of the trend that would be expected based on the retention volumes because, according to Eq. (7), the activity coefficient is inversely related to the specific retention volume. Thus, as the retention volume decreases, one might expect the activity coefficient to increase, indicating a lower amount of solute being absorbed into the stationary phase. However, the activity coefficient is also inversely related to the solute vapor pressure, which increases exponentially with temperature. As the vapor pressure above the liquid solvent phase increases, more of the solute vapor is partitioned into the solvent. Thus, the activity coefficient is dependent upon two competing parameters: the retention volume and the vapor pressure of the solute. Since the vapor pressure typically increases more rapidly at higher temperatures (exponentially), the vapor pressure effects will impact on the retention volume more at higher temperatures.

For methanol at 56.7 and 65.1 °C, the activity coefficient increases with temperature and then decreases as the temperature increases further. At this lower temperature, the increase in activity coefficient due to the specific retention volume dominates over the reduction in activity coefficient due to the vapor pressure. At temperatures beyond 65.1 °C, the activity coefficient diminishes with increasing temperature because the vapor pressure contribution dominates. The activity coefficients of the other three alcohols consistently decrease as temperature increases.

As the alcohol carbon number increases, the aliphatic nature of the solutes increases and the alcohol–biodiesel mixture behaves more ideally due to the chemical similarity between the solute and solvent. This is also reflected in that the activity coefficients decrease as the carbon number of the alcoholic solute increases.

4.4.2. Activity coefficients—comparisons with literature data

Similar trends are found from available activity coefficient data based on partition of alcoholic solutes into compounds chemically similar to biodiesel. The data from the study by Potts were determined using a soy-based biodiesel similar to the one used in this study but from a different manufacturer [44]. The DECHEMA data are based on alcoholic solutes interacting with octadeanoic acid, a long-chain fatty acid [52]. The Comanita et al. data are based on sorption of alcohols into ethyl octanoate [53]. The data are displayed in Fig. 2.

The experimental activity coefficient data from this study are typically a little lower than the data from DECHEMA. If the data from Comanita et al. are extrapolated into the temperature range

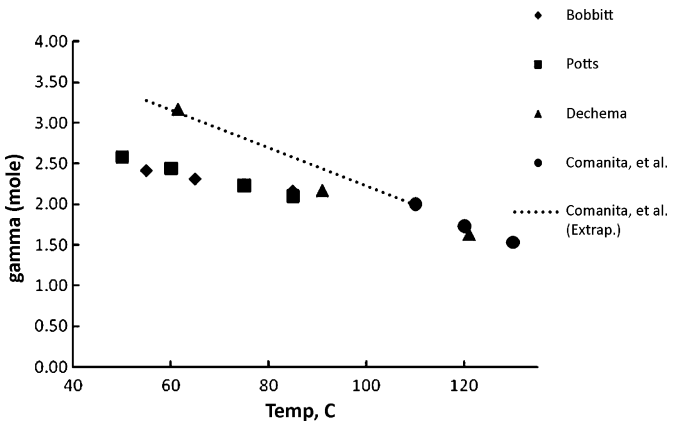

Fig. 2. Comparison of γ_x of ethanol in biodiesel as a function of temperature from this study with available literature data on biodiesel and model compound.

of this study, they would be slightly higher as well. The activity coefficient values from Potts are significantly lower for the methanol–biodiesel system but agree well for the other three alcohols. It was not expected that the activity coefficients would agree precisely with the data from DECHEMA and Comanita et al. because those literature values were for compounds similar to but not identical to biodiesel; however, the general agreement between these sources and the experimental data is satisfactory. It should also be noted that biodiesel from different sources or feed stocks (soya, rapeseed, corn, *et cetera*) will exhibit at least a slight variation in their solute biodiesel activity coefficients.

4.4.3. UNIFAC predictions

A modified UNIFAC software package provided by Sandler [54] was also used to predict activity coefficients for the binary systems under study. The model compound $CH_3(CH_2)_{16}CH_2COOH$ was used to approximate biodiesel's chemical composition due to lack of requisite information on the functional groups composing the biodiesel structure. Fig. 3(a–d) shows the predicted values and experimental values for each alcohol. It is evident that the UNIFAC predictions are consistently slightly higher than the experimentally determined values, but overall the agreement is gratifying, particularly for solutes methanol and ethanol.

4.4.4. Predictions based on regular solution theory

The Flory–Huggins (FH) and Miller–Guggenheim (MG) methods described by Martire [46,47] are two common methods of predicting the entropic activity coefficient, which are dependent upon ratios of molar volumes (Eqs. (11) and (12)). These methods can be coupled with predictions of the enthalpic activity coefficient from regular solution theory and used to predict the total mole fraction activity coefficient. These calculated results are reported and are compared with IGC-experimental data in Fig. 4(a–d). The two methods agree with each other within 6–7% differences, with the Miller–Guggenheim predicting consistently higher values for activity coefficients. Overall the agreement with experimental data is good. The predictions for methanol are typically lower than the experimental values, while the predictions for n-propanol and n-butanol are higher. The predictions for ethanol agree extremely well with the observed experimental values. With the exception of ethanol, the Flory–Huggins and Miller–Guggenheim predictions have better agreement with the experimental data at lower temperatures.

4.4.5. The Margules equation

A more rigorous method of predicting activity coefficients was also devised using the two-constant Margules equation (Eq. (13)).

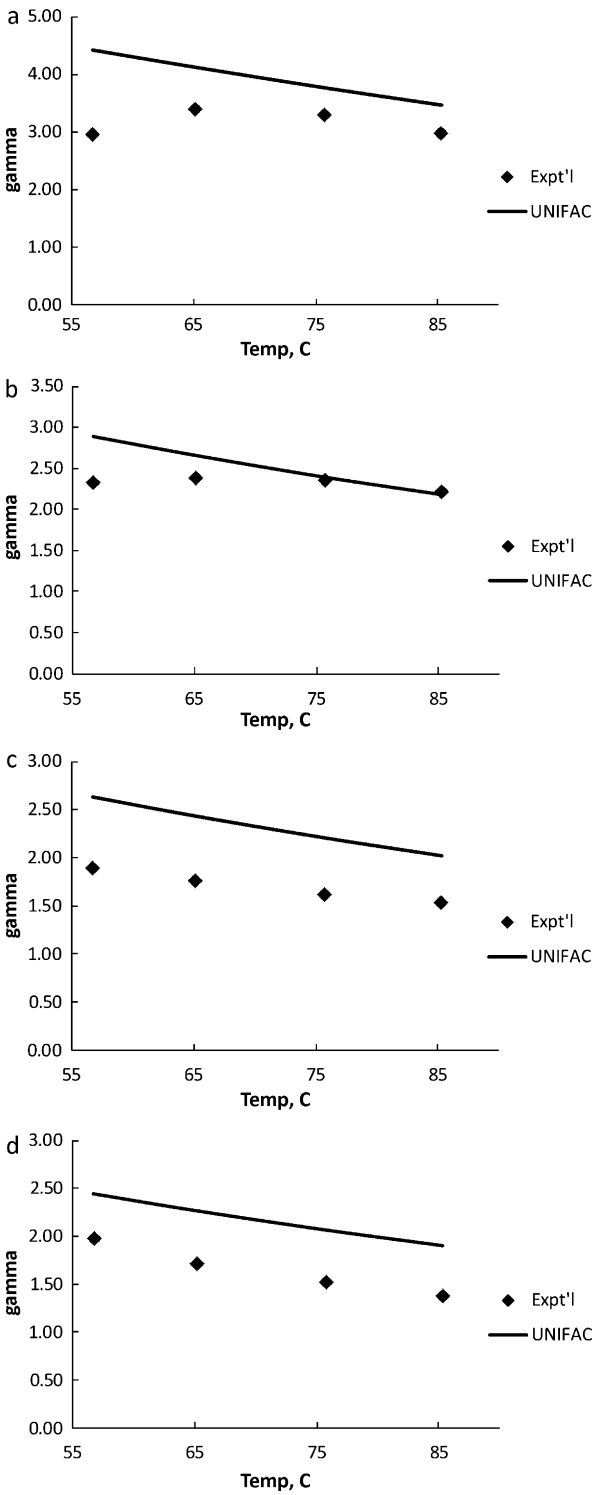

Fig. 3. (a) A comparison of IGC-derived γ_x for methanol in biodiesel as a function of temperature versus γ_x predicted using the UNIFAC model.(b) Comparison of the IGC-derived γ_x for ethanol in biodiesel as a function of temperature with those predicted by UNIFAC.(c) Comparison of IGC-derived γ_x for the n-propanol/biodiesel system as a function of temperature versus those predicted using UNIFAC.(d) The γ_x for the n-butanol/biodiesel system as determined by IGC as a function of temperature versus those predicted by UNIFAC.

Two Margules equations can be solved simultaneously using two carefully chosen data points to obtain the characteristic constants that allow prediction of activity coefficients at a given temperature. This was done using a software program called TK Solver® 5.0 (UTS, Inc., 2003). These constants can then be used to solve for the activity

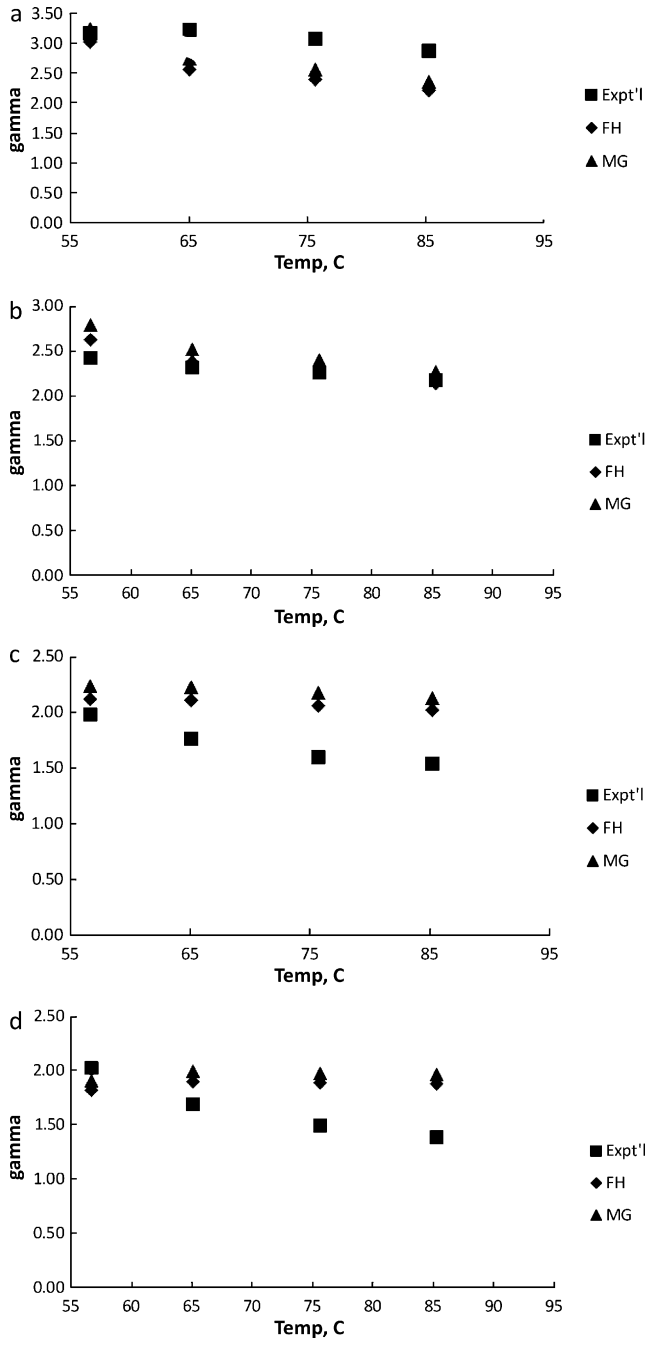

Fig. 4. (a) The γ_x for the methanol/biodiesel system predicted by the Flory–Huggins and Miller–Guggenheim equations as a function of temperature versus the experimentally derived IGC values.(b) The γ_x predicted for the ethanol/biodiesel system as a function of temperature by the Flory–Huggins and Miller–Guggenheim equations versus γ_x from IGC (this study).(c) Activity coefficients for the n-propanol/biodiesel system as a function of temperature predicted by the Flory–Huggins and Miller–Guggenheim equations versus γ_x derived from the IGC experiments.(d) The γ_x for the n-butanol/biodiesel system determined by IGC as a function of temperature versus those predicted by the Flory–Huggins and Miller–Guggenheim equations.

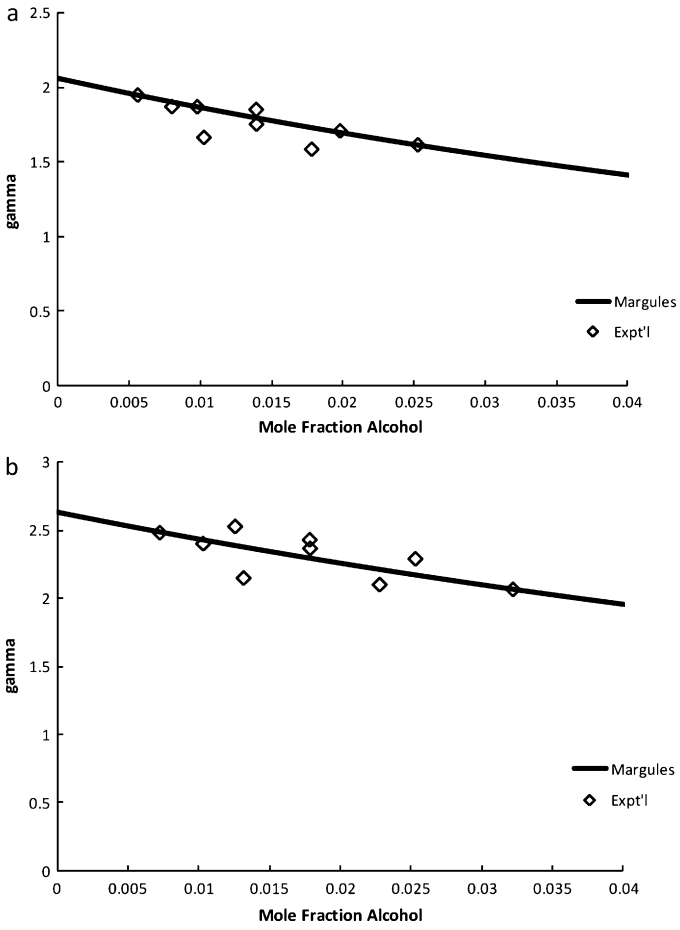

Fig. 5. (a) Margules equation predictions of the for the γ_x n-propanol/biodiesel system as a function of n-propanol mole fraction in biodiesel versus experimentally derived γ_x from IGC at 65 °C.(b) Activity coefficients for the ethanol/biodiesel system as a function of ethanol mole fraction in biodiesel; those predicted by the Margules equation versus IGC values at 65 °C.

coefficients of a binary alcohol–biodiesel mixture for any desired composition at that temperature. These parameters are tabulated in Table 6.

Fig. 5(a and b) shows the agreement between a curve generated from these Margules constants for ethanol and n-propanol at 65 °C and experimental data for the alcohol concentration ranges used in this study. The activity coefficient values calculated using the two-constant Margules equation with the constants reported in this study agree satisfactorily with the experimental data.

4.5. Solubility parameters

Fig. 6 shows that there is a linear relationship between solubility parameter and activity coefficients. It is noteworthy that these activity coefficients are reported for all four alcohols at four temperatures and the linear relationship holds, *id est* the relationship

Table 6
Margules equation constants regressed from experimental IGC data for the n-alcohols/biodiesel systems data.

Margules constants	56.7 °C		65.1 °C		75.7 °C		85.3 °C	
	A_{ij}	A_{ji}	A_{ij}	A_{ji}	A_{ij}	A_{ji}	A_{ij}	A_{ji}
Methanol	1.3369	−0.6295	1.3013	0.4573	1.2255	0.7703	1.1426	0.0886
Ethanol	1.1067	−4.0619	0.9667	−1.9978	0.8871	−0.7570	0.8183	−0.3195
Propanol	0.8801	−3.8385	0.7215	−3.5905	0.6524	−5.5262	0.5711	−3.9151
Butanol	0.9003	−6.1606	0.6976	−6.8423	0.5913	−7.4450	0.4929	−6.5372

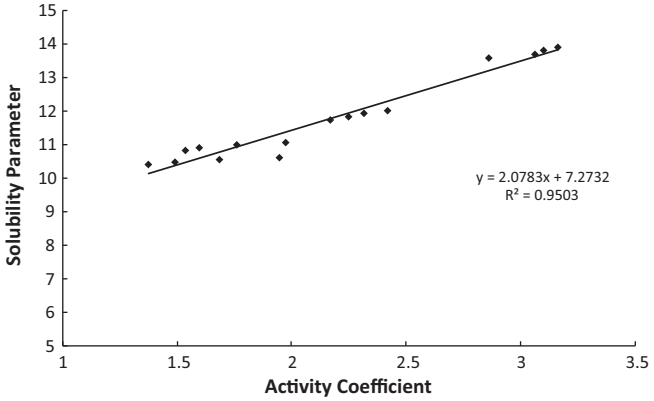

Fig. 6. Correlation between the n-alcohol (solute) solubility parameter vs. the n-alcohol (solute)–biodiesel activity coefficients determined by IGC.

between the solubility parameter and the activity coefficient is *independent of the solute species* for these solutes. Thus Fig. 6 can potentially be used to estimate the activity coefficient for a similar solute in biodiesel if the solubility parameter for that solute is known. The solubility parameter for soybean stock biodiesel has been calculated to be approximately 7.4–8.0 $(cal/cc)^{1/2}$ [34] so, as the solubility parameters of the solutes approach this value, the activity coefficients approach unity, indicating an increase in ideality of the solution in terms of enthalpic interactions, as predicted by regular solution theory.

4.6. Sorption isotherms

The sorption isotherms for the n-alcohol–methyl ester systems were calculated using the Elution by Characteristic Point method prescribed by Conder and Young (Eqs. (1) and (2)) [41]. These isotherms displayed less nonlinear behavior than was expected at the higher concentration of alcohol. The methanol– and ethanol–biodiesel systems displayed a slight Langmuir-type behavior that is more pronounced at higher temperatures. The higher carbon number alcohols (n-propanol, n-butanol) display similar trends. At the low end of the temperature range, n-propanol displays a very slight anti-Langmuir behavior that diminishes as temperature increases. At the highest temperature tested (85 °C) the isotherms for n-propanol and n-butanol are highly linear (R^2 value equal to 1). The n-butanol isotherms are significantly anti-Langmuir at 55 °C, and the degree of departure from a linear isotherm is reduced about 40% as the temperature increases to 85 °C. Overall, linear isotherms shift toward more Langmuir-type

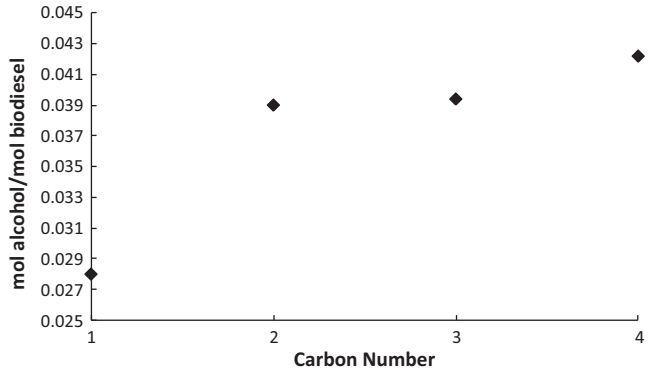

Fig. 7. Mole fraction ratio of n-alcohol/biodiesel vs. alcohol carbon number for 10 μL injections at 85 °C.

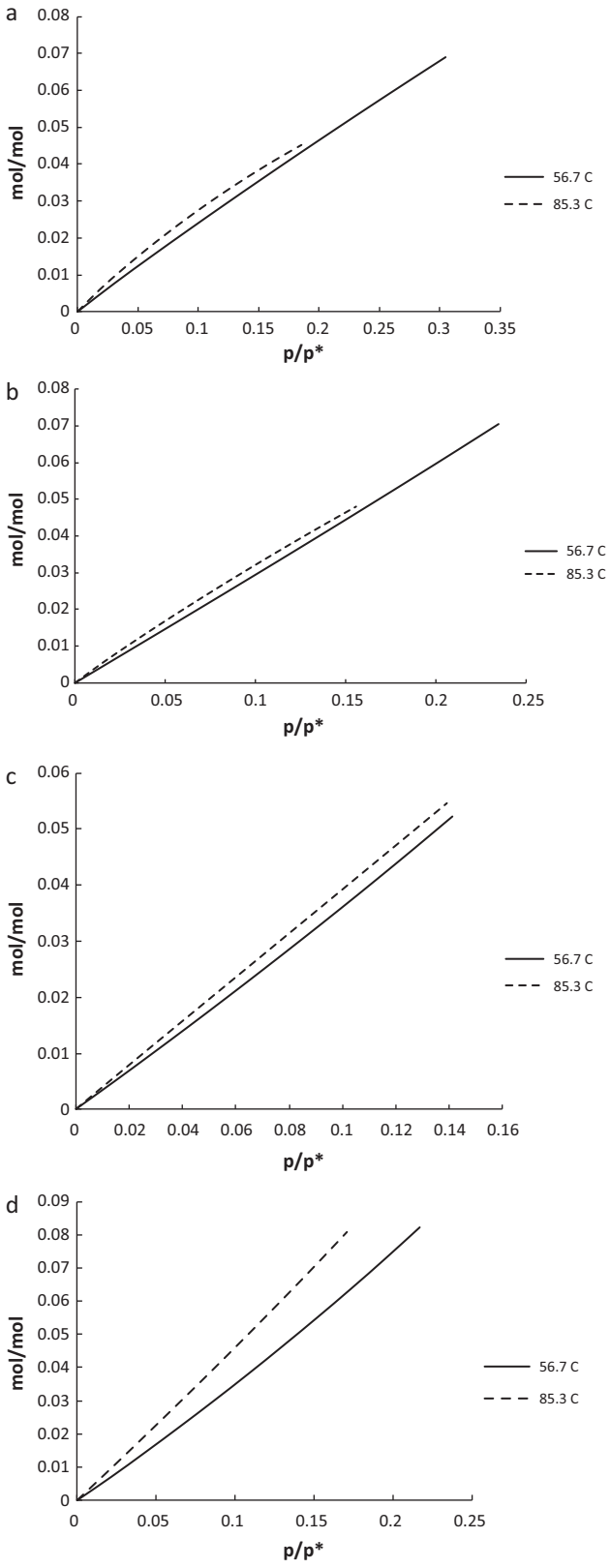

Fig. 8. (a) Methanol sorption isotherms on biodiesel at two temperatures (56.7 °C and 85.3 °C).(b) Ethanol uptake into biodiesel sorption isotherms at 56.7 °C and 85.3 °C.(c) Amount of n-propanol absorbed into biodiesel at two different temperatures (56.7 °C and 85.3 °C).(d) n-Butanol/biodiesel sorption isotherms at two different temperatures (56.7 °C and 85.3 °C)as a function of temperature.

behavior, and anti-Langmuir isotherms shift toward linear behavior as temperature increases. The opposite trend is observed as carbon number increases; *id est* linear isotherms shift toward anti-Langmuir-type behavior, and Langmuir isotherms shift toward linear behavior.

The amount of alcohol uptake by the biodiesel or absorption increases with the carbon number of the alcohol. This suggests that, as the carbon number increases, the alkyl nature of the alcohol makes a more dominant contribution to the molecular interactions with biodiesel and that the alcohol will mix more effectively with the biodiesel methyl esters, which also contain long, nonpolar hydrocarbon chains. Biodiesel is a primarily nonpolar solvent and mixes more readily with more nonpolar solutes, such as higher chain-length alcohols. Fig. 7 demonstrates the increase in solute absorption as the carbon chain is lengthened.

Fig. 8(a–d) displays the sorption isotherms for two temperatures for each of the studied alcohols. In the four examples pictured, the mole fraction uptake is plotted on the vertical axis, while the horizontal axis represents p/p^o, a measure of the vapor state concentration of the n-alcoholic solute. Overall for the stated solute vapor concentration range (p/p^o), the sorption isotherms maintain a high degree of linearity, exhibiting only slight deviations from Raoult's Law. This provides some confidence that solution thermodynamic parameters determined at near infinite dilution can be extrapolated into more finite concentration regions. The below sorption isotherms can be combined with Raoult's Law and the exhibited idealities or non-idealities from ideal solution behavior to allow process engineers to calculate the sorption of the designated alcoholic solutes in biodiesel for the concentration range approaching infinite dilution as indicated on the sorption isotherms provided.

5. Conclusion

The trends in the molar-based activity coefficients reflect a greater escaping tendency as temperature increases, with n-butanol having the lowest activity coefficient at all temperatures, indicating that n-butanol is preferentially absorbed into the biodiesel because of its nonpolar nature. Methanol has the highest activity coefficient in soy-based biodiesel and escapes more readily due to its high volatility and strongly polar nature. All n-alcohol solutes exhibit a positive deviation from Raoult's Law, indicating a preference for self-association as opposed to partition into the methyl ester solvent. These trends agree well with literature activity coefficient data on biodiesel and model compounds.

The trends in the Henry's Law coefficients corroborate the above inferences: the Henry's coefficients increase with temperature and decrease with carbon number of the alcohol, indicating that their escaping tendency or partial pressure above the biodiesel solution becomes greater as temperature increases and is lower as the n-alcohol chain is increased. Again, this is due to the preferential partitioning of the more nonpolar alcohols (n-propanol, n-butanol) into the predominantly nonpolar biodiesel solvent.

The partition coefficients are of interest for predicting chromatographic behavior and are inversely related to the distribution coefficients commonly used in chemical engineering calculations to measure the affinity of the solute for the (biodiesel) stationary phase. Such data on n-alcoholic solute interaction with biodiesel is of particular value in the design of engineering-scale operation, such as the distillation or centrifugal-based removal of alcohols from biodiesel solvents.

The sorption isotherms indicate an increased partitioning of alcohol into the biodiesel with increasing temperature, and also a greater affinity for biodiesel as the carbon number of the alcohols increases. These conclusions agree with the trends seen in the activity coefficient and partition coefficient data.

Acknowledgements

The authors gratefully acknowledge Teresa Alleman of the National Reneable Energy Laboratory for the biodiesel sample as well as Mr. Harold Watson and Dr. Keerthi Srinivas for technical assistance on certain aspects of this study.

References

[1] J.V. Gerpen, G. Knothe, in: G. Knothe, J. Krahl, J. van Gerpen (Eds.), The Basis of the Transesterification Reaction, The Biodiesel Handbook, AOCS Press, Champaign, IL, 2005, p. 26.
[2] V. Rudolph, Y. He, Dev. Chem. Eng. Miner. Process. 12 (5/6) (2004) 461.
[3] R.A. Peters, INFORM 7 (1996) 502.
[4] M.G. Pereira, S.M. Mudge, Chemosphere 54 (2004) 297.
[5] L. Adhami, B. Griggs, P. Himebrook, K. Taconi, J. Am. Oil Chem. Soc. 86 (2009) 1123.
[6] A. Voekel, B. Strzemiecka, K. Adamska, K. Milczewska, J. Chromatogr. A 1246 (2009) 1551.
[7] R.C. Castells, J. Chromatogr. A 1037 (2004) 223.
[8] M.D.A. Saldana, B. Tomberli, S.E. Guigard, S. Goldman, C.G. Gray, F. Temelli, J. Supercrit. Fluids 40 (2007) 7.
[9] H. Chen, AGasChromatographic Method to Determines Sorption Isotherms for Biomedical Polymers, Masters thesis, Texas Tech University, 1977.
[10] L. Bonifaci, L. Carnell, L. Cori, J. Appl. Polym. Sci. 51 (1994) 1923.
[11] A. Hadj-Ziane, S. Moulay, J.P. Canselier, J. Chromatogr. A 1091 (2005) 145.
[12] J.R. Galdamez, R.P. Danner, J.L. Duda, J. Chromatogr. A 1157 (2007) 399.
[13] D. Cava, J.M. Lagaron, F. Martinez-Gimenez, R. Gavara, J. Chromatogr. A 1175 (2007) 267.
[14] A.B. Nastasovic, A.E. Onjia, J. Chromatogr. A 1195 (2008) 1.
[15] N.V. Gwala, N. Deenadayalu, K. Tumba, D. Ramjugernath, J. Chem. Thermodyn. 42 (2010) 256.
[16] A.W. Lantz, V. Pino, J. Anderson, D.W. Armstrong, J. Chromatogr. A 1115 (2006) 217.
[17] F. Mutelet, J.-N. Jaubert, J. Chromatogr. A 1102 (2006) 256.
[18] A. Marchiniak, M. Wlazo, J. Chem. Eng. Data 55 (2010) 3208.
[19] M.-L. Ge, L.-S. Wang, J. Chem. Eng. Data 53 (2008) 846.
[20] Y.G. Dobryakov, D. Tuma, G. Mauer, J. Chem. Eng. Data 53 (2008) 2154.
[21] E. Papier, H. Balard, A. Vidal, Eur. Polym. J. 24 (1988) 316.
[22] J.M. Kaltenecker-Commercon, T.C. Ward, J. Adhesion 42 (1993) 113.
[23] V. Swaminathan, J. Cobb, I. Saracovan, Int. J. Pharm. 312 (2006) 158.
[24] T. Hamieh, J. Schultz, J. Chromatogr. A 969 (2002) 17.
[25] T. Hamieh, S. Abdessater, J. Toufaily, J. Phys. IV France 124 (2005) 37.
[26] G. Buckton, H. Gill, Adv. Drug Deliv. Rev. 59 (2007) 1474.
[27] O. Ferreira, G.M. Foco, Lat. Am. Appl. Res. 33 (2003) 257.
[28] P. Alessi, I. Kikic, A. Cortesi, Ind. Eng. Chem. Res. 41 (2002) 4873.
[29] J. Zhou, R. Yu, S. Wu, Z. Xie, Y. Yang, Ind. Eng. Chem. Res. 49 (2010) 1691.
[30] E. Diaz, S. Ordonez, A. Vega, J. Phys.: Conf. Ser. 61 (2007) 904.
[31] M. Przybyszewska, A. Krzywania, M. Zaborski, M.I. Szymkowska, J. Chromatogr. A 1216 (2009) 5284.
[32] J.W. King, G.R. List, J. Am. Oil Chem. Soc. 67 (1990) 424.
[33] J.W. King, Lebensm.-Wiss u.-Technol. 28 (1995) 190.
[34] K Srinivas, T.M. Potts, J.W. King, Green Chem. 11 (2009) 1581.
[35] C.-W. Chiu, M.J. Goff, G.J. Suppes, AIChE J. 51 (2005) 1274.
[36] R.D. Felice, D.D. Faveri, P.D. Andreis, P. Ottonello, Ind. Eng. Chem. Res. 47 (2008) 7862.
[37] W. Zhou, D.G.B. Boocock, J. Am. Oil Chem. Soc. 83 (2006) 1047.
[38] G.P. Silva, E.G. Lima Neto, S.S. Almeida, N.A. Costa, II Iberoamerican Conference on Supercritical Fluids PROSCIBA, Natal,Brazil, 2010.
[39] H. Kuramochi, K. Maeda, S. Kato, M. Osako, K. Nakamura, S. Sakai, Fuel 88 (2009) 1472.
[40] M.B. Oliveira, A.J. Queimada, J.A.P. Coutinho, Ind. Eng. Chem. Res. 49 (2010) 1419.
[41] J.R. Conder, C.L. Young, Physicochemical Measurement by Gas Chromatography, John Wiley & Sons, 1979.
[42] J.W. King, Surface Chemistry Studies by Gas Chromatography, Ph.D. thesis, Northeastern University, 1973.
[43] K.L. Mallik, An Introduction to Nonanalytical Applications of Gas Chromatography, The Peacock Press, New Delhi, 1976.
[44] T.M. Potts, Measurement of Solution Thermodynamic Properties of Mtehylsoyate/Solvent Systems by Inverse Gas Chromatography, Masters thesis, University of Arkansas, 2009.
[45] A.J. Ashworth, D.H. Everett, Trans. Faraday Soc. 56 (1960) 1609.
[46] D.E. Martire, in: L. Fowler (Ed.), Gas Chromatography: Analysis Instrumentation Division of the Instrument Society of America, Academic Press, 1963.
[47] D.E. Martire, in: A.B. Littlewood (Ed.), Gas Chromatography, The Elsevier Publishing Company, 1966, p. 21.

[48] G.M. Kontogerorgis, G.K. Folas, Thermodynamic Models for Industrial Applications, John Wiley & Sons, 2010.
[49] J.M. Smith, H.C. Van Ness, M.M. Abbott, Chemical Engineering Thermodynamics, Tata McGraw-Hill Publishing Company Limited, 2004.
[50] A. Levy, J. Sci. Instrum. 41 (1964) 449.
[51] R.E. Tate, K.E. Watts, C.A.W. Allen, K.I. White, Fuel 85 (2006) 1004.
[52] D. Tiegs, J. Gmehling, A. Medina, M. Soares, J. Bastos, A.P.I. Kikic, DECHEMA, Schön & Wetzel GmbH, 1986, p. 706.
[53] V.J. Comanita, R.A. Greenkorn, K.-C. Chao, J. Chem. Eng. Data 21 (1976) 491.
[54] S. Sandler, UNIFAC Software, Student Resource CD to Accompany Chemical, Biochemical, and Engineering Thermodynamics, 4th ed., John Wiley & Sons, 2006.